Circuits Syst Signal Process (2018) 37:3903–3926
https://doi.org/10.1007/s00034-018-0746-3

Sensitivity and Variability Analysis for Image Denoising Using Maximum Likelihood Estimation of Exponential Distribution

Amita Nandal[1] · Arvind Dhaka[2] · Hamurabi Gamboa-Rosales[3] · Ninoslav Marina[1] · Jorge I. Galvan-Tejada[3] · Carlos E. Galvan-Tejada[3] · Arturo Moreno-Baez[3] · Jose M. Celaya-Padilla[4] · Huizilopoztli Luna-Garcia[3]

Received: 4 July 2017 / Revised: 1 January 2018 / Accepted: 5 January 2018 /
Published online: 19 January 2018

Abstract In this paper, we have performed denoising when the pixel values of images are corrupted by Gaussian and Poisson noises. This paper introduces a new class exponential distribution which lies between Poisson and Gamma distributions. The proposed method combines the ion for denoising the pixels and later a minimization

✉ Amita Nandal
amita_nandal@yahoo.com

Arvind Dhaka
arvind.neomatrix@gmail.com

Hamurabi Gamboa-Rosales
hamurabigr@uaz.edu.mx

Ninoslav Marina
nonislav.marina@gmail.com

Jorge I. Galvan-Tejada
gatejo@uaz.edu.mx

Carlos E. Galvan-Tejada
ericgalvan@uaz.edu.mx

Arturo Moreno-Baez
morenob20@uaz.edu.mx

Jose M. Celaya-Padilla
jose.celaya@uaz.edu.mx

Huizilopoztli Luna-Garcia
hlugar@uaz.edu.mx

1 Universty of Information Science and Technology, Ohrid, Macedonia

2 National Institute of Technology, Hamirpur, India

3 Faculty of Electrical Engineering, Autonomous University of Zacatecas, Zacatecas, Mexico

4 CONACYT - Autonomous University of Zacatecas, Zacatecas, Mexico

Birkhäuser

using log-likelihood estimation is performed. The characteristic equation is based on various image parameters like mean, variance, mean deviation, distortion index, shape and scale parameters for minimizing the noise and for maximizing image edge strength to enhance overall visual quality of the image. By utilizing the exponential distribution, we can adaptively control the distortion in the image by minimizing Gaussian and Poisson noises in accordance with the image feature. The simulation results indicate that the proposed algorithm is very efficient to strengthen edge information and remove noise. To provide a probabilistic model we have used statistical approximation of mean and variances. Later, we have evaluated sensitivity and variability effect as well on the image restoration. Experiments were conducted on different test images, which were corrupted by different noise levels in order to assess the performance of the proposed algorithm in comparison with standard and other related denoising methods.

Keywords Exponential distribution · Gamma-distributed noise · Image denoising · Log-likelihood estimation · Poisson-distributed noise · Sensitivity · Statistical estimation and variability

1 Introduction

The ever-increasing demand of pixel sensors is an evident of the importance of digital imaging in various applications [20,37]. Generally, the pixel sensor measurements follow Poisson distribution. There are various methods that are based on shrinking the pixel sensor size, increasing the image resolution at the cost of the need for denoising the Poisson-corrupted images [9,23,27,28]. The presence of the noise in any imagery degrades the spatial and contrast resolution. The noise distribution can vary from Gaussian, Gamma, Poisson, or it can follow some compound distribution as well. The signal-to-noise ratio scales linearly with the Poisson intensity which is a main challenge in digital imaging [37]. Moreover, the approximation of Poisson-induced noise in images follows different models which makes image denoising algorithms to be designed for Gaussian noise. However, each resolution cell of the noise-affected image has multiple numbers of scatterers that return randomly distributed signals and cause poor visual interpretation [13]. In this paper, we have used exponential distribution [15,19] approach to model the log-likelihood estimator [8,22] for denoising with the advantages of approximate mean deviation, better sensitivity, better variability, and perfect reconstruction with minimized distortion index.

In all applications, the images are ultimately viewed by human beings, and therefore, every denoising algorithm must quantify visual image quality through subjective evaluation. Generally, subjective evaluation is too time-consuming and expensive process [16]. The simplest and most widely used quality metrics are peak signal-to-noise ratio (PSNR) and mean-squared error (MSE), computed by averaging the squared intensity differences of noise-induced and reference image pixels. Another important metric discussed in this paper is structural similarity (SSIM) that compares local patterns of pixel intensities that have been normalized for exposure and contrast. These parameters are mathematically convenient in the context of optimization [10,11,41,42,45]. We present experimental results from a set of three images and have compared the results among various denoising methods. Since we have considered the Poisson- and Gamma-related noise which is comparable to Bayesian-based estimation methods available in the literature [3,14,17,26,32,38,47,49].

In this paper, the closed-form expressions to estimate the distortion parameter-based sensitivity and variability are derived for an uncorrupted image by minimizing the distortion. The parameters involved in the proposed method have been estimated using statistical approach with log-likelihood estimation. The uncorrupted image has been maximized for noise-free image pixels in accordance with log-likelihood estimator by employing an exponential distribution for the vectors of image with and without noise effect. This paper proposes an adaptive estimation method based on the variable exponent which gives a good estimate for Poisson- and Gamma-affected images. We have used the shape, scale, contrast, exposure, distortion, and edge strength parameters in the proposed method. The proposed method restores an image successfully by controlling the small features effectively. To assess the performance of the proposed method based denosing, we have used log-likelihood estimation. We have assessed the performance of proposed method before applying log-likelihood which is termed as proposed method before log-likelihood (PBL) and proposed method after applying log-likelihood estimation which is termed as proposed method after log-likelihood (PL).

The organisation of the paper is as follows: Sect. 2 describes the literature review. The proposed methodology is explained in Sect. 3. The performance measures are described in Sect. 4. The experimental results of the proposed method are discussed in Sect. 5. Finally, Sect. 5 concludes the paper.

2 Literature Review

In the literature, various noise reduction techniques are discussed such as resolution enhancement approach, averaging approach, and post-processing approach using filters and sliding window to estimate the statistical information of all pixels using the local mean and local variance [12,31,50]. Multiscale processing is the most commonly used approach in Poisson image denoising models [5]. Latest developments in this area include biased mean estimators and unbiased estimate of risk which recovers noise-free wavelet coefficients [4]. It has been shown that effective signal reconstruction can be achieved by employing shrinkage factor based on Bayesian formalism than by using the thresholding techniques [4,36]. In [36], parameters of the mixed exponential distribution are estimated using fractional moments. We have used exponential distribution with log-likelihood approximation in the proposed method. The irregularities in Poisson data can be treated in various ways. For Poisson noise and multiplicative Gamma noise, the Bayesian maximum a posterior (MAP) likelihood estimation is presented in the literature [18,24,33,35,44,48]. These methods follow simple model for image restoration in the presence of Poisson and multiplicative noises. But these existing methods for image restorations are designed specifically for a given type of noise, while our model can handle image restoration with mixed and unknown distribution of noises. We have compared our proposed approach with the methods presented in [24,35]. In [24] noise of varying scales is being removed, while preserving low-contrast features in regions of low intensity which is termed as contrast-based denoising (CBD). In [35] a variational restoration model (VRM) for removing multiplicative Gamma noise is proposed using Douglas–Rachford splitting techniques. But, uniform regularization strength must be chosen to either remove high-intensity noise or to retain low-intensity features; both cannot be done using this approach. These models are not adaptive for different noise distributions, which is the advantage of our proposed method. This paper presents a novel exponential distribution using log-likelihood estimator for image denoising. A new family of exponential distribution lies between Gamma and Poisson distribution and is designed to fit the observed likelihood approximation. In our proposed method, we have used sensitivity and variation indices to offer a robust approach for exploiting the correlation and variance in any imagery for better visual quality. We have compared the test results of different image quality assessment against three sets of images with 128×128 pixels and 512×512 pixels.

3 Proposed Method

Statistical modeling is very important aspect in fields of scientific study and others. There are various statistical models with different type of response variables based on likelihood paradigm. Some very important generalized linearized models include Gaussian, Gamma, Binomial, Poisson. All these models belong to the exponential dispersion models (EDM) [2,46]. We have used an intermediate model between Gaussian and Poisson distributions to evaluate first two moments, i.e., mean and variance. The variance function describes the relationship between mean and variance of response variable. The block diagram for the proposed algorithm is shown in Fig. 1. Consider random variable Y with mean μ and variance $\phi\mu^p$ such that, $\phi > 0, p \in (-\infty, 0] \cup [1, \infty)$ which describes $Y = \mathrm{EDM}_p(\mu, \phi)$. The mean is $E(Y) = \mu$ and variance is written as $\mathrm{Var}(Y) = \phi V(\mu) = \phi\mu^p$. $\mathrm{EDM}_p(\mu, \phi)$ is an exponential dispersion model (EDM) of two variables μ and ϕ. For $p = 0$ the EDM is Gaussian, for $p = 1, \phi = 1$ the EDM is Poisson, for $p = 2$, $p = 3$ the EDM is Gamma and inverse Gaussian and for $1 < p < 2$ the EDM becomes compound Poisson distribution. The probability density function (PDF) of EDM is evaluated using numerical methods available in literature [2]. We assume that the pixel space in the image is denoted by (i, j), where we considered $i, j = 1, 2 \ldots n$ and $n = 128$ or 512. Assume that W_{ij} is a vector to be considered for all noise-free pixel values. N_{ij} is a vector that include all pixels with noise $\left(X_{ij}\right)$ and without noise $\left(W_{ij}\right)$ such that $N_{ij} = W_{ij} + X_{ij}$. The noise density is represented as σ_X which is considered as 10, 20, 30, 40 and 50 in this paper. It is assumed that all the pixels are independent and their PDFs are Poisson-distributed. X_{ij} is independent with Poisson- and Gamma-distributed noise with mean τ_{ij}. According to [46], N_{ij} follows an exponential compound Poisson model. The distribution of N_{ij} can also be re-parameterized in such a way that it takes the form of the exponential family such that scale parameter (p) is a function of edge strength sharpness parameter (v) as

$$p = \frac{v + 2}{v + 1}, p \in (1, 2), v > 0. \tag{1}$$

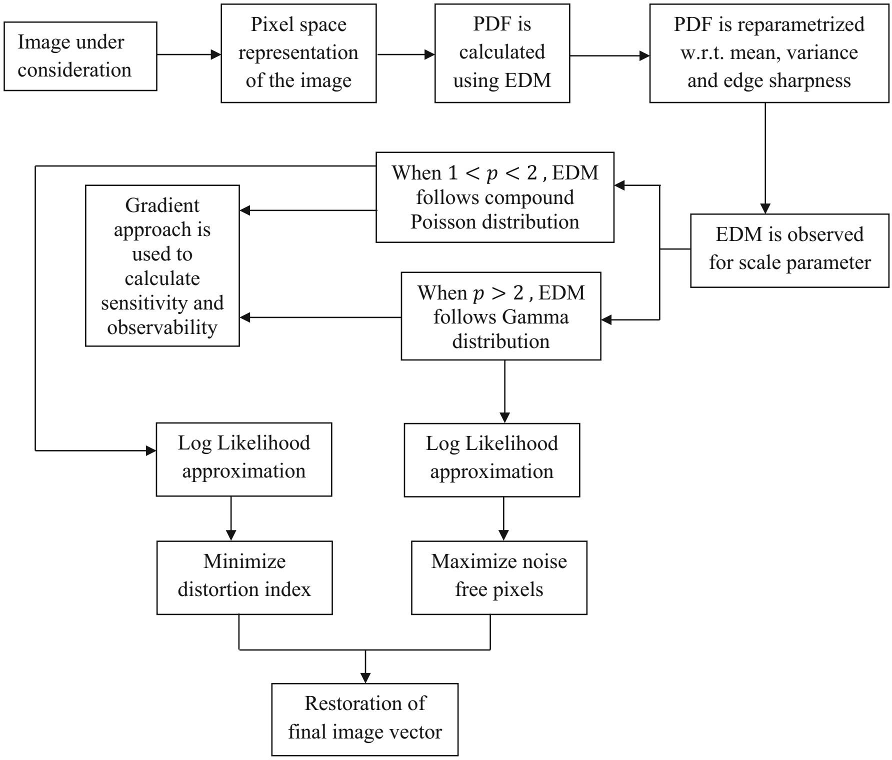

Fig. 1 Block diagram of the proposed algorithm

Overall mean $\left(\mu_{ij}\right)$ is multiplicative in nature such that $\mu_{ij} = \lambda_{ij}\tau_{ij}$. λ_{ij} is the mean of noise-free pixels. Distortion index is defined as,

$$\phi_{ij} = \frac{\lambda_{ij}^{1-p}\tau_{ij}^{2-p}}{(2-p)}. \tag{2}$$

Here the probability of pixels affected by noise is zero. The probability density function [46] is written as

$$P(N_{ij}=0) = \exp\left(-W_{ij}\lambda_{ij}\right) = \exp\left(\frac{W_{ij}}{\phi_{ij}}\left(-k_p\left(\phi_{ij}\right)\right)\right). \tag{3}$$

For the probability that pixels affected by noise is greater than zero, the probability density function [46] is

$$f\left(\lambda_{ij}, \tau_{ij}, v\right) = C\left(\frac{W_{ij}}{\phi_{ij}}; p\right)\exp\left(\frac{W_{ij}}{\phi_{ij}}\left(N_{ij}(\theta) - k_p(\theta)\right)\right). \tag{4}$$

$C\left(\frac{W_{ij}}{\phi_{ij}}; p\right)$ is a constant which is a function of noise-free pixels and scale parameter. It is evaluated using Gamma function [46]. Here θ is the deviation in the mean,

$\theta = \begin{cases} \frac{\mu^{1-p}}{1-p}, p \neq 1 \\ \log \mu, p = 1 \end{cases}$. The exposure and contrast operator (k) in form of a cumulating generating function [2] is written as $k = \frac{1}{2-p}\left((1-p)\theta\right)^{\frac{2-p}{1-p}}$. k can be represented in terms of μ as

$$k = \begin{cases} \frac{\mu^{2-p}}{2-p}, & p \neq 2 \\ \log\mu, & p = 2 \end{cases}. \tag{5}$$

$C\left(\frac{W_{ij}}{\phi_{ij}}; p\right)$ is to be evaluated numerically which is a constant which has been analyzed for two cases in this paper. It is defined with the help of gamma distribution as

$$C\left(\frac{W_{ij}}{\phi_{ij}}; p\right) = \sum\nolimits_{i,j=1}^{n} \frac{1}{i!j!\Gamma\left(vW_{ij}\right)} \left(\frac{W_{ij}^{v}\left(\frac{W_{ij}}{\phi_{ij}}\right)^{v+1}}{(p-1)^{v}(2-p)}\right). \tag{6}$$

Here $\Gamma(.)$ is Gamma function. N_{ij} has mean μ_{ij}, ϕ_{ij} is the dispersion parameter. k is the exposure and contrast operator with p as scale parameter. $p \to 1$ for over dispersed Poisson distribution and $p \to 2$ for Gamma distribution. Our model is a bridge between Poisson and Gamma models, i.e., $P \in (1, 2)$. We will now calculate the constant function for these two cases.

Case 1 When $1 < p < 2$ then constant function $C\left(\frac{W_{ij}}{\phi_{ij}}; P\right)$ in Eq. (4) becomes

$$C\left(\frac{W_{ij}}{\phi_{ij}}; p\right) = \frac{W_{ij}^{-\alpha}(p-1)^{\alpha}}{\phi_{ij}^{(1-\alpha)}(2-p)^{\alpha}\, i!j!\Gamma(-\alpha)}. \tag{7a}$$

Here is shape parameter [2,46] such that $\alpha = \frac{(2-p)}{(1-p)}$. By substituting Eq. (7) in (4), we get density function as

$$f\left(\lambda_{ij}, \tau_{ij}, v\right) = \frac{W_{ij}^{-\alpha}(p-1)^{\alpha}}{\phi_{ij}^{(1-\alpha)}(2-p)^{\alpha}\, i!j!\Gamma(-\alpha)}.\exp\left(\frac{W_{ij}}{\phi_{ij}}\left(N_{ij}(\theta) - k_p(\theta)\right)\right). \tag{7b}$$

Case 2 When $p > 2$ then constant function $C\left(\frac{W_{ij}}{\phi_{ij}}; p\right)$ in Eq. (4) becomes

$$C\left(\frac{W_{ij}}{\phi_{ij}}; p\right) = \frac{1}{\pi\left(W_{ij}\right)^{\alpha}\left(f\left(\lambda_{ij}, \tau_{ij}, v\right)\right)}. \tag{8}$$

After substituting probability function in terms of Gamma function and simplifying above equation, we get

$$C\left(\frac{W_{ij}}{\phi_{ij}};p\right)=\frac{\Gamma\left(1+\alpha\right)\phi^{(\alpha-1)}\left(p-1\right)^{\alpha}}{\left(W_{ij}\right)^{\alpha}.\Gamma\left(1+\alpha\right)\left(p-2\right)^{\alpha}y^{\alpha}}.\left(-1\right)^{\alpha}\sin\left(-\pi\alpha\right) \quad . \tag{9a}$$

By substituting Eq. (9) in (4), we get density function as

$$\begin{aligned} & f\left(\lambda_{ij},\tau_{ij},v\right) \\ & =\frac{\Gamma\left(1+\alpha\right)\phi^{(\alpha-1)}\left(p-1\right)^{\alpha}}{\left(W_{ij}\right)^{\alpha}.\Gamma\left(1+\alpha\right)\left(p-2\right)^{\alpha}y^{\alpha}}.\left(-1\right)^{\alpha}\sin\left(-\pi\alpha\right) \\ & \quad .\exp\left(\frac{W_{ij}}{\phi_{ij}}\left(N_{ij}\left(\theta\right)-k_{p}\left(\theta\right)\right)\right). \end{aligned} \tag{9b}$$

Equations (7b) and (9b) are the equations for the probability density functions for the proposed method evaluated using exponential dispersion family of distributions. These PDFs are observed w.r.t. compound Poisson model and Gamma model to analyze sensitivity and variability using gradient approach as discussed in subsequent section.

3.1 Sensitivity and Variability Analysis

Now we estimate sensitivity and variability as a function of (ϕ, p). We have used quasi-score function [21] and Pearson estimating function [1] with distortion and scale parameters. As mentioned that scale parameter provides edge strength information. Therefore, scale parameter will be useful in restoring edge information. The image sensitivity function is quasi-score function [21] of (ϕ, p) which is written as

$$\psi\left(\phi,p\right)=\nabla\mu_{ij}C^{-1}\left(N_{ij}-\mu_{ij}\right). \tag{10}$$

The sensitivity matrix (S) of ψ is a $n\times n$ matrix which is written as $S=E\left(\nabla\psi\right)$. The variability matrix (V) of ψ is a $n\times n$ matrix which is written as $V=\mathrm{Var}\left(\psi\right)$. Using Pearson function [1], we can write $\psi\left(\phi,p\right)$ as

$$\psi\left(\phi,p\right)=N_{ij}^{T}W_{ij}-tr\left(W_{ij}C^{-1}\right). \tag{11}$$

We evaluate sensitivity and variability matrix by finding derivatives of ψ w.r.t. ϕ and p. The $(n\times n)$ sensitivity matrix w.r.t. ϕ and p is given by

$$S\left(\phi\right)=E\left(\frac{\delta\psi\left(\phi,p\right)}{\delta\phi}\right), \tag{12a}$$

$$S\left(p\right)=E\left(\frac{\delta\psi\left(\phi,p\right)}{\delta p}\right). \tag{12b}$$

Here $\frac{\delta C}{\delta\phi}=\mathrm{diag}\left(\mu^{p}\right)$ and $\frac{\delta C}{\delta p}=\mathrm{diag}\left(\phi\log\left(\mu\right)\mu^{p}\right)$. We can show using results about characteristic function of linear and quadratic forms of non-normal variables [21] such that the entries in variability matrix is given by

$$V\left(\phi\right)=2tr\left(N_{ij}\left(W_{ij}C\right)\right)+\sum\nolimits_{k}k\left(N_{ij}\right)^{\phi}\left(W_{ij}\right)^{\phi}, \tag{13a}$$

$$V\left(p\right)=2tr\left(N_{ij}\left(W_{ij}C\right)\right)+\sum\nolimits_{k}k\left(N_{ij}\right)^{p}\left(W_{ij}\right)^{p}. \tag{13b}$$

To take into account the correlation matrix between vector ϕ and p, we need to compute cross-sensitivity and cross-variability matrix [40]. The entries of cross-sensitivity matrix (CS) between ϕ and p are given by

$$\mathrm{CS}\left(\phi,p\right)=-tr\left(C^{-1}\frac{\delta C}{\delta\phi}.C^{-1}\frac{\delta C}{\delta p}\right). \tag{14}$$

Finally, we the cross-variability matrix (CV) between ϕ and p is given by

$$\mathrm{CV}\left(\phi,p\right)=2tr\left(N_{ij}\left(W_{ij}C\right)\right)+\sum\nolimits_{i,j=1}^{n}k\left(N_{ij}\right)^{\phi}\left(W_{ij}\right)^{p}. \tag{15}$$

The sensitivity and variability analyses are an accurate way to predict the visual quality of image and image is more pleasant when cross-sensitivity (Eq. 14) and cross-variability (Eq. 15) correlation approaches to 1.0. We have also observed effect its effect on sensitivity and variability on the images under consideration. The sensitivity value is high when the noise effect is reduced and the variability value is more when noise effect is more. From Eq. (12a, 12b), it is observed that sensitivity and variability follow gradient approach w.r.t. distortion and scale parameter. Also, it is mentioned that scale parameter affects the edge strength. The values obtained for sensitivity and variability at different noise densities, i.e., $\sigma = 10, 20, 30, 40$ and 50. The average of three images is summarized in Tables 1 and 2, respectively, for $1 < p < 2$ and $p > 2$. The overall determinant of matrix $S(\phi)$ represents sensitivity w.r.t. distortion and the overall determinant of matrix $S(p)$ represents sensitivity w.r.t. edge strength. So, the sensitivity value should be high. The overall determinant of matrices $V(\phi)$ represents variability w.r.t. distortion, and the overall determinant of matrix $V(p)$ represents variability w.r.t. edge strength. So, the variability value should be low. Another important observation here is the correlation sensitivity ($\mathrm{CS}(\phi, p)$) and correlation variability ($\mathrm{CV}(\phi, p)$) which should be close to 1 for better visual quality.

3.2 The Likelihood Function and Optimization of Distortion Parameter

The probability function $f\left(\lambda_{ij}, \tau_{ij}, v\right)$ is an exponential probability density function. The log-likelihood function [29,30] for an image size $n \times n$ is given by

$$l\left(N_{ij},\phi_{ij},p\right)=\sum\nolimits_{i,j=1}^{n}\log f\left(\lambda_{ij},\tau_{ij},v\right). \tag{16}$$

We can maximize this equation w.r.t. ϕ_{ij}. There are various methods [1,2,21] for maximization process. By substituting $f\left(\lambda_{ij}, \tau_{ij}, v\right)$ from Eq. (4), we get

$$l\left(N_{ij},\phi_{ij},p\right)=\sum\nolimits_{i,j=1}^{n}\log\left(C\left(\frac{W_{ij}}{\phi_{ij}},p\right)\right)+\frac{W_{ij}}{\phi_{ij}}\left(N_{ij}\frac{\mu_{ij}^{1-p}}{1-p}-\frac{\mu_{ij}^{2-p}}{2-p}\right). \tag{17}$$

Table 1 Calculated values for sensitivity from average of three image sets

$S(\phi)$, $S(p)$	$1 < p < 2$, Poisson-distributed noise				$p > 2$, Gamma-distributed noise			
	CS $(\phi, p) = 0.1$	CS $(\phi, p) = 0.3$	CS $(\phi, p) = 0.6$	CS $(\phi, p) = 0.9$	CS $(\phi, p) = 0.1$	CS $(\phi, p) = 0.3$	CS $(\phi, p) = 0.6$	CS $(\phi, p) = 0.9$
128×128 *pixel size*								
$\sigma_X = 10$	89	112	142	249	78	88	109	137
$\sigma_X = 20$	81	102	129	227	71	80	99	124
$\sigma_X = 30$	73	92	116	204	64	72	89	112
$\sigma_X = 40$	66	83	105	185	58	65	81	101
$\sigma_X = 50$	51	65	83	146	45	51	63	79
512×512 *pixel size*								
$\sigma_X = 10$	122	154	195	342	107	121	150	188
$\sigma_X = 20$	111	140	177	311	97	110	136	170
$\sigma_X = 30$	100	126	159	280	88	99	122	154
$\sigma_X = 40$	91	114	144	254	80	89	111	139
$\sigma_X = 50$	70	89	114	200	62	70	86	108

Table 2 Calculated values for variability from average of three image sets

$V(\phi)$, $V(p)$	$1 < p < 2$, Poisson-distributed noise				$p > 2$, Gamma-distributed noise			
	CV $(\phi, p) = 0.1$	CV $(\phi, p) = 0.3$	CV $(\phi, p) = 0.6$	CV $(\phi, p) = 0.9$	CV $(\phi, p) = 0.1$	CV $(\phi, p) = 0.3$	CV $(\phi, p) = 0.6$	CV $(\phi, p) = 0.9$
128×128 *pixel size*								
$\sigma_X = 10$	163	93	73	58	89	71	58	51
$\sigma_X = 20$	207	118	93	74	113	91	73	65
$\sigma_X = 30$	228	130	103	82	125	100	81	72
$\sigma_X = 40$	253	144	114	91	139	111	90	80
$\sigma_X = 50$	278	159	125	100	153	122	99	88
512×512 *pixel size*								
$\sigma_X = 10$	218	122	95	73	116	92	73	64
$\sigma_X = 20$	278	156	122	96	150	119	95	84
$\sigma_X = 30$	306	172	136	107	166	131	105	93
$\sigma_X = 40$	342	192	151	119	185	146	118	104
$\sigma_X = 50$	375	212	166	131	204	162	130	114

Here the distortion index is written as

$$\phi_{ij} = \frac{-\sum_{i,j=1}^{n} W_{ij}\left(N_{ij}\frac{\mu_{ij}^{1-p}}{1-p} - \frac{\mu_{ij}^{2-p}}{2-p}\right)}{(1-v)\sum_{i,j} N_{ij}}. \tag{18}$$

It can be estimated by maximum likelihood estimator by setting minimum and maximum values for ϕ_{ij}. This is achieved by substituting the derivative of Eq. (17) equal to zero. By adjusting the number of parameters, we get the distortion index as:

$$\phi_{ij} = \phi = \sum_{i,j} \frac{2}{N-Q}\left(N_{ij}\left(\frac{N_{ij}^{1-p} - \mu_{ij}^{1-p}}{1-p} - \frac{N_{ij}^{2-p} - \mu_{ij}^{2-p}}{2-p}\right)\right). \tag{19}$$

N denotes total number of pixels. Q is the number of pixels used in estimating the distortion. Variance parameters have an impact on the mean parameter and vice-versa. p, ϕ and W_{ij} have impact on variance of the model and less on mean. When we use the likelihood principle for estimating ϕ, we minimize the vector with pixels affected by noise. We will calculate the derivatives of W_{ij} w.r.t. ϕ. Later, we have optimized using log-likelihood criterion. By differentiating $f\left(\lambda_{ij}, \tau_{ij}, v\right)$ w.r.t. ϕ, we get

$$\frac{\delta \log f\left(\lambda_{ij}, \tau_{ij}, v\right)}{\delta\phi} = \begin{cases} \frac{\mu^{2-p}}{\phi^2(2-p)}, & y = 0 \\ \frac{N_{ij}\mu^{1-p}}{\phi_{ij}^2(p-1)} + \frac{\mu^{2-p}}{\phi_{ij}^2(2-p)} + \frac{\delta N_{ij}}{N_{ij}\delta\phi}, & y > 0 \end{cases}. \tag{20}$$

Case 1 When $1 < p < 2$ then differentiating W_{ij} w.r.t. ϕ, we get

$$\frac{\delta W_{ij}}{\delta\phi} = \sum_{i,j=1}^{n} C\left(\frac{W_{ij}}{\phi_{ij}}; p\right) W_{ij}, \tag{21a}$$

Using log-likelihood estimation,

$$\frac{\delta \log\left(W_{ij}\right)}{\delta\phi} \approx \phi\,(1-\alpha) - \log(2\pi) - \frac{1}{2}\log(-\alpha)\,. \tag{21b}$$

Now in order to maximize W_{ij}, the derivative is set equal to zero. To do this W_{ij} is written in form of a gamma function as

$$\log\left(W_{ij}\right) = \phi \log\left(\frac{N_{ij}^{-\alpha}\,(p-1)^{\alpha}}{\phi^{1-\alpha}\,(2-p)}\right) - \log\Gamma\,(1+\phi) - \log\Gamma\,(-\alpha\phi)\,. \tag{22}$$

Now replace the gamma function by Stirling approximation [1] and approximating $(1-\alpha\phi)$ and $(-\alpha\phi)$ gives

$$\log\left(W_{ij}\right) \approx \phi\left\{\log\left(\frac{N_{ij}^{-\alpha}\,(p-1)^{\alpha}}{\phi^{1-\alpha}\,(2-p)}\right) + (1-\alpha) + \alpha\log(-\alpha) - (1-\alpha)\log\phi\right\}$$
$$-\log(2\pi) - \frac{1}{2}\log(-\alpha) - \log\phi. \tag{23}$$

$\alpha < 0$ for $1 < p < 2$, so logarithms have positive arguments. Differentiating Eq. (23) w.r.t. ϕ,

$$\frac{\delta\log\left(W_{ij}\right)}{\delta\phi} \approx \log\left(\frac{N_{ij}^{-\alpha}\,(p-1)^{\alpha}}{\phi^{1-\alpha}\,(2-p)}\right) - \frac{1}{\phi} - \log\phi + \alpha\log(-\alpha\phi). \tag{24}$$

$\frac{\delta\log(W_{ij})}{\delta\phi} = 0$ at $\phi_{\text{opt}} = \frac{N_{ij}^{2-p}}{(2-p)\phi}$. This approximation is good for maximum value of W_{ij} which is found as by substituting ϕ_{opt} in maximum likelihood equation as

$$\max(\log W_{ij}) = \phi_{\text{opt}}\,(\alpha-1) - \log(2\pi) - \log\left(\phi_{\text{opt}}\right) - \frac{1}{2}\log(-\alpha). \tag{25}$$

Case 2 When $p > 2$ then differentiating W_{ij} w.r.t. ϕ we get

$$\frac{\delta W_{ij}}{\delta\phi} = \sum\nolimits_{i,j=1}^{n} C\left(\frac{W_{ij}}{\phi_{ij}}; p\right) W_{ij}, \tag{26a}$$

Approximating $k \approx \frac{\mu^{2-p}}{\phi(p-2)}$ and using log-likelihood estimation, we get

$$\frac{\delta\log\left(W_{ij}\right)}{\delta\phi} \approx (1-\alpha)\,k + \frac{1}{2}\log(\alpha) + \log(k). \tag{26b}$$

Now in order to maximize W_{ij} the derivative is set equal to zero. To do this W_{ij} is written in form of a gamma function as

$$W_{ij} = \frac{\left(\frac{(p-1)^{\alpha}\phi^{\alpha-1}}{N_{ij}^{\alpha}(p-2)}\right)^{k}\Gamma(1+\alpha k)}{\Gamma(1+k)}. \tag{27}$$

By Stirling approximation [1],

$$\log\left(W_{ij}\right) \approx k\left[\log\left(\frac{(p-1)^{\alpha}\,\phi^{\alpha-1}}{N_{ij}^{\alpha}\,(p-2)}\right) + (1-\alpha)\right.$$
$$\left. -\log(k) + \alpha\log(\alpha k)\right] + \frac{1}{2}\log(\alpha). \tag{28}$$

$\frac{\delta \log(W_{ij})}{\delta\phi} = 0$ at $\phi_{\text{opt}} = \frac{N_{ij}^{p-2}}{(p-2)\phi}$. This approximation is good for maximum value of W_{ij} which is found by substituting ϕ_{opt} in maximum likelihood equation as

$$\max(\log W_{ij}) = k\left[\phi_{\text{opt}}\,(1-\alpha) - \log(k) - \log\left(\phi_{\text{opt}}k\right)\right] + \frac{1}{2}\log(\alpha)\,. \tag{29}$$

Thus, the final output image $\left(N_{ij_{\text{final}}}\right)$ is restored from the vector of the maximized values from the noise-free image where distortion index ϕ is minimized.

4 Performance Measures

The proposed method was tested on three image sets each with resolution of 128 × 128 pixels and 512 × 512 pixels. For each image, noisy observation is generated by adding the Gaussian- and Gamma-distributed noise with original image having standard deviation of 10, 20, 30, 40, and 50 dB. All the simulations have been carried out on MATLAB R2013a on a 2.67GHz i5 processor. Mean square error (MSE), peak signal-to-noise ratio (PSNR), mean absolute error (MAE), structural similarity index metric (SSIM), image quality index (QI), and time taken during simulation are used to benchmark denoising performance.

Mean square error is computed here as parametric estimation error. Parametric error reflects the uncertainty in reliability of estimates. One good estimate is established in [25,46] of exponential compound Poisson model as,

$$\begin{aligned}\text{MSE}[N_{ij}] = {} & \sum\nolimits_{ij} \phi W_{ij}\mu_{ij}^{1} + \sum(W_{ij}\mu_{ij})^2\text{Var}[X_{ij}\beta] \\ & + \sum\nolimits_{ij\in\forall(i1,\,j1\neq i2,\,j2)}(W_{i1}\mu_i 1)(W_{i2}\mu_i 2)\cdots(W_{ij}\mu_{ij}) \\ & \cdot\sum\nolimits_{ij\in\forall(i1,\,j1\neq i2,\,j2)}\text{Cov}(X_i 1\beta,\, X_{ij}\beta)\text{Cov}(X_1 j\beta,\, X_{ij}\beta).\end{aligned} \tag{30}$$

$\text{Cov}\left(X_{i1}\beta, X_{ij}\beta\right)$ is the corresponding covariance matrix elements.

PSNR and mean absolute error (MAE) are used to measure the quality of restoration results. Mathematically PSNR is given by

$$\text{PSNR} = 10\log\left(\frac{255^2 n^2}{\left|N_{ij} - N_{ij_{\text{final}}}\right|^2}\right)\text{dB}. \tag{31}$$

Here, N_{ij} is the original image and $N_{ij_{\text{final}}}$ is the final restored output denoised image. Mean absolute error is written as,

$$\text{MAE} = \frac{\left|N_{ij} - N_{ij_{\text{final}}}\right|}{n^2}. \tag{32}$$

PSNR can tell how well the reconstruction data match the true data and the data which is not required to restore image. PSNR can measure the intensity difference between

Table 3 Calculated values K_W w.r.t. number of pixels

	Image set 1	Image set 2	Image set 3
$T = 100$	0.578	0.612	0.595
$T = 300$	0.672	0.702	0.611
$T = 500$	0.718	0.713	0.705

two images. Therefore, it may not be reliably used to describe visual perception of image. So, PSNR is accurate measure for restoration of edges. We have evaluated another important visual quality assessment performance measure which is SSIM. Mathematically,

$$\mathrm{SSIM} = \frac{1}{n}\sum\nolimits_{i,j=1}^{n} \frac{\left(2\mu_{N_{ij\mathrm{final}}}\mu_{N_{ij}} + c_1\right)\left(2\sigma_{N_{ij\mathrm{final}}} + c_2\right)}{\left(\mu^2_{N_{ij\mathrm{final}}} + \mu^2_{N_{ij}} + c_1\right)\left(\sigma^2_{N_{ij\mathrm{final}}} + \sigma^2_{N_{ij}}\right)}. \tag{33}$$

$\mu_{N_{ij\mathrm{final}}}$, $\mu_{N_{ij}}$ are the mean associated with output image and noise-induced original image, respectively. $\sigma^2_{N_{ij\mathrm{final}}}$ and$\sigma^2_{N_{ij}}$ are the variance associated with output image and noise-induced original image, respectively. The noise density for noisy pixels is given by σ_X such that

$$\sigma_X = \frac{1}{n-1}\sum\nolimits_{i,j=1}^{n}\left(N_{ij} - \mu_W\right)\left(N_{ij} - \mu_{ij\mathrm{final}}\right). \tag{34}$$

The values of constants are chosen as $c_1 = 0.01$ and $c_2 = 0.03$ [25]. The large value of SSIM depicts better performance.

Image quality index (QI) is another parameter for visual quality assessment. Mathematically,

$$QI = \frac{4\sigma_{N_{ij}}\sigma_{N_{ij\mathrm{final}}}\mu_{N_{ij}}\mu_{N_{ij\mathrm{final}}}}{\left(\sigma^2_{N_{ij}} + \sigma^2_{N_{ij\mathrm{final}}}\right)\left(\mu^2_{N_{ij}} + \mu^2_{N_{ij\mathrm{final}}}\right)}. \tag{35}$$

The value of image quality index should be between 0 and 1. The best value is 1. This parameter includes the effect due to loss of correlation, luminance, and contrast distortion. For accuracy assessment we have used the way to measure accuracy by using statistical technique [34]. In order to access the overall accuracy, Cohen [39] defined most widely used statistics for the estimation of the effect of change agreement called Kappa Statistic. The overall accuracy is given as $O_{\mathrm{acc}} = \sum_{i,j=1}^{n} \frac{N_{ij}}{T}$. Here, T is the number of pixels considered. The value of T can be considered as any value between $1, 2 \ldots 512$. In our experiments the value of T is taken for 100, 300 and 500. The Kappa factor for image free pixels is $K_W = \frac{O_{\mathrm{acc}} - p_W}{1 - p_W}$. Here, $p_W = \frac{\sum_{i,j=1}^{n} W_{ij}^2}{n}$ is the statistic of pixels without noise. The ideal value of Kappa factor should be 1. The values for K_W are given in Table 3.

4.1 Computational Complexity

We have evaluated the computational complexity [6,7,43] for proposed method and compared it with the methods available in literature. The computational complexity of CBD method [24] has three parts. First part calculates pixelated Poisson noise with complexity of $O\left(n2^n\right)$. The second part computes the prior distribution with complexity $O\left(2^{2n}\left(n\right)^{O(n)}\right)$. The third part consists of the computational load related to minimization using Euler Lagrange equation and its computational complexity is $O\left(2n^2\right)$. Therefore, the overall complexity becomes $O\left(n2^n\right)+O\left(2^{2n}\left(n\right)^{O(n)}\right)+O\left(2n^2\right)$. The computational complexity of VRM method [35] is also divided into three parts. The first part includes calculation of discrete denoising model using gradient approach with computational complexity of $nO\left(n\right)$. The second part calculates conjugate function using variational method with computational load of $O\left(n^2\log n\right)$. The third part calculates the minimization function using Douglas–Rachford splitting with computational complexity of $nO\left(2n\right)$. Thus, the overall complexity can be written as $nO\left(n\right)+O\left(n^2\log n\right)+nO\left(2n\right)$. The proposed method without likelihood estimation has computational complexity $O\left(n^2\log n\right)+nO\left(n\right)$. The first part computes PDF using EDM and the second part is for computations related to sensitivity and variability using gradient approach. The log-likelihood evaluation has additional computational complexity $nO\left(\log\left(1+2n\right)\right)$. Therefore, proposed method with likelihood estimation has computational complexity of $O\left(n^2\log n\right)+nO\left(n\right)+nO\left(\log\left(1+2n\right)\right)$. We have tabulated the computational time in seconds in experimental results as well. It is observed that though the computational time using proposed method is comparable to the state of art methods under comparison and the visual quality of image is better as illustrated from different performance metrics.

5 Results and Discussion

In the our experiments, we evaluated the effect of the proposed method on denoising performance. In these experiments, three images contaminated by Poisson and Gamma noises at different noise densities 10, 20, 30, 40, and 50 are used. The overall performance was quantified on a set of three images. Figures 2, 3, 4, 5, 6, and 7 show the resulting images for each denoising methods for different values of noise densities. It is observed that the visual quality of the proposed estimator is superior to other methods. Also, we have observed that proposed method without log-likelihood estimation provides performances slightly inferior in terms of SNR as compared to proposed method with log-likelihood estimation. Figures 2, 3 and 4 show the images with 128×128 pixel space and Figs. 5, 6 and 7 are for the images 512×512 pixel space. The proposed method exhibit a good performance in restoring geometrical structures of the images. We have observed that Poisson noise is minimized effectively when $1<p<2$. For the case when $p>2$, the distribution is more close to gamma distribution so it can be used when Gamma and inverse Gaussian noise are present in the input image. The proposed algorithm is better both visually and quantitatively as revealed by performance measures. It has been satisfied that using log-likelihood estimator the noise can be minimized using the proposed methodology. The presented

(a) (b) (c) (d) (e)

Fig. 2 Qualitative results for noise density $\sigma_X = 10$ for 128×128 pixel size. **a** Noisy image, **b** CBD [24], **c** VRM [35], **d** PBL, **e** PL

(a) (b) (c) (d) (e)

Fig. 3 Qualitative results for noise density $\sigma_X = 30$ for 128×128 pixel size. **a** Noisy image, **b** CBD [24], **c** VRM [35], **d** PBL, **e** PL

(a) (b) (c) (d) (e)

Fig. 4 Qualitative results for noise density σ_X $\sigma_X = 50$ for 128×128 pixel size. **a** Noisy image, **b** CBD [24], **c** VRM [35], **d** PBL, **e** PL

(a) (b) (c) (d) (e)

Fig. 5 Qualitative results for noise density σ_X $\sigma_X = 10$ for 512×512 pixel size. **a** Noisy image, **b** CBD [24], **c** VRM [35], **d**, PBL, **e** PL

approximation gives better results when the choice of the parameters is appropriate. Simulation results indicate that proposed method is able to reconstruct edges and restores the contrast very well. The noise minimized image attains the largest PSNR. The denoising performance results for MSE are (Eq. 30) given in Tables 4 and 5 for 128×128 and 512×512 pixels space, respectively. Various other performance measures are evaluated in Tables 6, 7, 8 and 9 such as PSNR (Eq. 31), MAE (Eq. 32), SSIM (Eq. 33), QI (Eq. 35) and computational time in seconds in respect of the computational complexity. The PSNR improvement brought by our approach is quite high and the visual resolution is quite remarkable. Moreover, the new algorithm with log-likelihood estimation is better than without log-likelihood estimation. It is observed that when distortion index and noise density decrease, the image quality improves. The obtained PSNR results indicate that the proposed method has better performance

Fig. 6 Qualitative results for noise density $\sigma_X = 30$ for 512×512 pixel size. **a** Noisy image, **b** CBD [24], **c** VRM [35], **d** PBL, **e** PL

Fig. 7 Qualitative results for noise density $\sigma_X = 50$ for 512×512 pixel size. **a** Noise image, **b** CBD [24], **c** VRM [35], **d** PBL, **e** PL

than others, especially at low SNRs. In our experiment, the same set of images is taken with different pixel size and noise contaminations. The obtained results for various performance measures at different noise levels are summarized in Tables 4, 5, 6, 7, 8 and 9. From the obtained results we can conclude that the proposed denoising algorithm outperforms as compared to the other methods for all noise intensity situations. When looking closer at the results, we observe that using the proposed method PSNR is improved by 19%, MAE is improved by 32% and SSIM is improved by 10% as compared to [24,35] for different noise densities. The values of these parameters have been tabulated for different values for noise density as 10, 20, 30, 40 and 50 for both cases, i.e., $1 < p < 2$ and $p > 2$. We have shown the results for small (128×128) and big (512×512) pixel space images. It is observed that even, for big size images the proposed method takes almost comparable time as taken for small size images. The proposed method outperforms other methods by resulting in more pleasant visual image. It is observed that even at high-intensity noise, all PSNR values and quality measure image quality index of our method are higher.

Conclusion

In this paper, based on the exponential distribution function, we have proposed an adaptive image denoising model using log-likelihood approximation. In our method, we have used the mean, variance, distortion index, scale parameter, sensitivity, and variability analysis as the variable exponent to analyze and control image quality. Compared with the other methods, using the proposed method the quality of restored images is quite well. We proposed the minimization of noise using log-likelihood estimation for multiscale Poisson and Gamma induced noises in image. The denoising operation is effective to restore the image features and contrast. This paper shows that an exponential denoiser based on the log-likelihood estimation under suitable

Table 4 Calculated MSE values for 128 × 128 pixel size using proposed method after log-likelihood estimation

	$1 < p < 2$, Poisson-distributed noise				$p > 2$, Gamma-distributed noise			
	$\phi = 1$	$\phi = 0.1$	$\phi = 0.01$	$\phi = 0.001$	$\phi = 1$	$\phi = 0.1$	$\phi = 0.01$	$\phi = 0.001$
Image set 1								
$\sigma_X = 10$	20.512	15.012	12.134	11.157	25.323	18.533	14.980	13.774
$\sigma_X = 20$	30.132	26.132	21.143	15.129	37.201	32.262	26.102	18.678
$\sigma_X = 30$	30.153	35.132	30.148	20.152	49.572	43.373	37.220	24.879
$\sigma_X = 40$	30.151	36.183	30.132	20.156	41.915	43.609	37.200	24.884
$\sigma_X = 50$	30.192	36.191	33.152	25.132	41.965	43.878	37.743	25.373
Image set 2								
$\sigma_X = 10$	16.615	12.160	9.829	9.037	19.271	14.321	11.731	10.851
$\sigma_X = 20$	24.407	21.167	17.126	12.255	27.929	24.329	19.839	14.426
$\sigma_X = 30$	32.524	28.457	24.420	16.323	36.948	32.429	27.943	18.947
$\sigma_X = 40$	33.622	32.548	24.407	16.326	45.946	36.975	27.929	18.950
$\sigma_X = 50$	33.656	32.598	36.573	18.457	45.983	36.919	28.447	20.429
Image set 3								
$\sigma_X = 10$	13.668	10.003	8.085	7.434	15.853	11.781	9.650	8.927
$\sigma_X = 20$	20.078	17.413	14.089	10.081	22.976	20.014	16.320	11.868
$\sigma_X = 30$	26.756	23.410	20.089	13.428	30.395	26.678	22.987	15.587
$\sigma_X = 40$	33.418	26.776	20.078	13.431	37.797	30.417	22.976	15.590
$\sigma_X = 50$	33.445	33.398	21.087	14.410	37.828	33.775	24.096	16.678

Table 5 Calculated MSE values for 512 × 512 pixel size using proposed method after log-likelihood estimation

	$1 < p < 2$, Poisson-distributed noise				$p > 2$, Gamma-distributed noise			
	$\phi = 1$	$\phi = 0.1$	$\phi = 0.01$	$\phi = 0.001$	$\phi = 1$	$\phi = 0.1$	$\phi = 0.01$	$\phi = 0.001$
Image set 1								
$\sigma_X = 10$	22.369	16.371	13.232	12.167	27.615	20.210	16.336	15.021
$\sigma_X = 20$	32.859	28.497	23.057	16.498	40.568	35.182	28.465	20.369
$\sigma_X = 30$	32.882	38.312	32.877	21.976	54.059	47.299	40.589	27.131
$\sigma_X = 40$	32.880	39.458	32.859	21.980	45.709	47.556	40.567	27.136
$\sigma_X = 50$	32.925	39.467	36.153	27.407	45.763	47.850	41.159	27.670
Image set 2								
$\sigma_X = 10$	19.303	14.127	11.419	10.499	22.389	16.638	13.629	12.606
$\sigma_X = 20$	28.356	24.591	19.897	14.238	32.447	28.265	23.049	16.760
$\sigma_X = 30$	37.786	33.061	28.371	18.964	42.925	37.675	32.464	22.012

Table 5 continued

	$1 < p < 2$, Poisson-distributed noise				$p > 2$, Gamma-distributed noise			
	$\phi = 1$	$\phi = 0.1$	$\phi = 0.01$	$\phi = 0.001$	$\phi = 1$	$\phi = 0.1$	$\phi = 0.01$	$\phi = 0.001$
$\sigma_X = 40$	39.061	37.814	28.356	18.967	53.379	42.957	32.447	22.016
$\sigma_X = 50$	39.101	37.872	42.490	21.443	53.422	42.892	33.049	23.734
Image Set 3								
$\sigma_X = 10$	15.018	10.991	8.884	8.168	17.419	12.945	10.603	9.809
$\sigma_X = 20$	22.061	19.133	15.481	11.077	25.246	21.991	17.932	13.040
$\sigma_X = 30$	29.399	25.722	22.073	14.754	33.397	29.313	25.258	17.127
$\sigma_X = 40$	36.719	29.421	22.061	14.758	41.531	33.422	25.246	17.130
$\sigma_X = 50$	36.749	36.697	23.170	15.833	41.565	37.111	26.476	18.325

Table 6 Performance measures as average of three image sets for $1 < p < 2$, $\phi = 1$ and $k = 1$ with different noise densities

	128 × 128 pixel size					512 × 512 pixel size				
	$\sigma_X = 10$	$\sigma_X = 20$	$\sigma_X = 30$	$\sigma_X = 40$	$\sigma_X = 50$	$\sigma_X = 10$	$\sigma_X = 20$	$\sigma_X = 30$	$\sigma_X = 40$	$\sigma_X = 50$
PSNR										
CBD [24]	38.532	34.845	32.701	31.182	30.791	42.718	38.631	36.254	34.570	34.136
VRM [35]	40.675	39.873	35.673	35.013	32.093	45.094	44.205	39.549	38.817	35.580
PBL	43.765	42.156	40.162	39.134	39.092	48.520	46.736	44.525	43.386	43.339
PL	47.896	46.982	45.914	44.983	44.883	53.100	52.086	50.902	49.870	49.759
MAE										
CBD [24]	4.132	5.321	6.121	7.185	9.413	3.727	4.800	5.521	6.481	8.491
VRM [35]	4.912	5.012	5.927	7.232	8.613	4.431	4.521	5.346	6.523	7.769
PBL	3.012	3.136	4.127	4.912	5.013	2.717	2.829	3.723	4.431	4.522
PL	2.698	2.517	3.131	3.511	4.017	2.434	2.270	2.824	3.167	3.623
SSIM										
CBD [24]	96.012	91.927	87.742	83.743	71.932	106.443	101.915	97.275	92.841	79.747
VRM [35]	98.104	92.176	86.762	80.141	73.153	108.763	102.191	96.188	88.848	81.101
PBL	102.863	96.918	90.564	85.132	80.893	114.039	107.448	100.404	94.381	89.682
PL	106.715	101.982	92.893	89.013	86.091	118.309	113.062	102.986	98.684	95.445
QI										
CBD [24]	0.932	0.901	0.893	0.852	0.813	0.940	0.909	0.901	0.860	0.821
VRM [35]	0.921	0.912	0.842	0.801	0.792	0.929	0.920	0.850	0.809	0.800
PBL	0.942	0.932	0.901	0.901	0.891	0.950	0.940	0.909	0.909	0.899
PL	0.972	0.963	0.957	0.942	0.931	0.980	0.971	0.965	0.950	0.939

Table 6 continued

	128 × 128 pixel size					512 × 512 pixel size				
	$\sigma_X = 10$	$\sigma_X = 20$	$\sigma_X = 30$	$\sigma_X = 40$	$\sigma_X = 50$	$\sigma_X = 10$	$\sigma_X = 20$	$\sigma_X = 30$	$\sigma_X = 40$	$\sigma_X = 50$
Time (s)										
CBD [24]	55.262	60.661	70.771	76.912	80.153	49.846	54.716	63.835	69.375	72.298
VRM [35]	56.261	60.173	71.621	78.924	81.153	50.747	54.276	64.602	71.189	73.200
PBL	58.132	62.153	73.158	76.986	82.351	52.435	56.062	65.989	69.441	74.281
PL	59.141	62.197	73.874	77.012	83.132	53.345	56.102	66.634	69.465	74.985

Table 7 Performance measures as average of three image sets for $p > 2$, $\phi = 1$ and $k = 1$ with different noise densities

	128 × 128 pixel size					512 × 512 pixel size				
	$\sigma_X = 10$	$\sigma_X = 20$	$\sigma_X = 30$	$\sigma_X = 40$	$\sigma_X = 50$	$\sigma_X = 10$	$\sigma_X = 20$	$\sigma_X = 30$	$\sigma_X = 40$	$\sigma_X = 50$
PSNR										
CBD [24]	34.533	31.228	29.307	27.946	27.595	37.741	34.129	32.029	30.542	30.159
VRM [35]	36.453	35.735	31.970	31.379	28.762	39.840	39.054	34.940	34.294	31.434
PBL	39.223	37.781	35.994	35.072	35.035	42.866	41.290	39.337	38.330	38.289
PL	42.925	42.106	41.149	40.314	40.225	46.912	46.017	44.971	44.059	43.961
MAE										
CBD [24]	3.013	3.880	4.463	5.239	6.864	3.293	4.240	4.878	5.726	7.501
VRM [35]	3.582	3.655	4.322	5.273	6.280	3.914	3.994	4.723	5.763	6.864
PBL	2.196	2.287	3.009	3.582	3.655	2.400	2.499	3.289	3.914	3.995
PL	1.967	1.835	2.283	2.560	2.929	3.150	3.006	2.995	2.798	2.201
SSIM										
CBD [24]	85.875	82.221	78.478	74.901	64.337	93.852	89.859	85.768	81.859	70.314
VRM [35]	87.746	82.444	77.601	71.680	65.429	95.897	90.103	84.810	78.338	71.507
PBL	92.002	86.685	81.002	76.144	72.352	100.549	94.738	88.527	83.217	79.073
PL	95.448	91.215	83.085	79.615	77.001	104.315	99.688	90.803	87.011	84.154
QI										
CBD [24]	0.920	0.889	0.881	0.840	0.801	0.940	0.909	0.901	0.860	0.821
VRM [35]	0.909	0.900	0.830	0.789	0.780	0.929	0.920	0.850	0.809	0.800
PBL	0.930	0.920	0.889	0.889	0.879	0.950	0.940	0.909	0.909	0.899
PL	0.960	0.951	0.945	0.930	0.919	0.980	0.971	0.965	0.950	0.939
Time (s)										
CBD [24]	40.214	44.143	51.500	55.969	58.327	43.950	48.244	56.284	61.168	63.746
VRM [35]	40.941	43.788	52.119	57.433	59.055	44.745	47.856	56.960	62.768	64.541
PBL	42.303	45.229	53.237	56.023	59.927	46.233	49.430	58.183	61.227	65.494
PL	43.037	45.261	53.758	56.042	60.495	47.035	49.465	58.752	61.248	66.115

Table 8 Performance measures as average of three image sets for $1 < p < 2$, $\phi = 1$ and $k = 0.5$ with different noise densities

	128 × 128 pixel size					512 × 512 pixel size				
	$\sigma_X = 10$	$\sigma_X = 20$	$\sigma_X = 30$	$\sigma_X = 40$	$\sigma_X = 50$	$\sigma_X = 10$	$\sigma_X = 20$	$\sigma_X = 30$	$\sigma_X = 40$	$\sigma_X = 50$
PSNR										
CBD [24]	31.211	28.224	26.488	25.257	24.941	34.602	31.291	29.366	28.002	27.650
VRM [35]	32.947	32.297	28.895	28.361	25.995	36.526	35.806	32.035	31.442	28.820
PBL	35.450	34.146	32.531	31.699	31.665	39.301	37.856	36.065	35.143	35.105
PL	38.796	38.055	37.190	36.436	36.355	43.011	42.190	41.231	40.395	40.305
MAE										
CBD [24]	5.101	6.569	7.557	8.870	11.621	4.601	5.926	6.816	8.001	10.483
VRM [35]	6.064	6.188	7.317	8.928	10.633	5.470	5.581	6.600	8.053	9.591
PBL	3.719	3.872	5.095	6.064	6.189	3.354	3.493	4.596	5.470	5.583
PL	3.331	3.107	3.865	4.335	4.959	3.005	2.802	3.486	3.910	4.473
SSIM										
CBD [24]	77.770	74.461	71.071	67.832	58.265	86.219	82.551	78.793	75.201	64.595
VRM [35]	79.464	74.663	70.277	64.914	59.254	88.098	82.775	77.912	71.967	65.692
PBL	83.319	78.504	73.357	68.957	65.523	92.372	87.033	81.327	76.449	72.642
PL	86.439	82.605	75.243	72.101	69.734	95.830	91.580	83.419	79.934	77.310
QI										
CBD [24]	0.911	0.880	0.872	0.831	0.792	0.919	0.888	0.880	0.839	0.800
VRM [35]	0.900	0.891	0.821	0.780	0.771	0.908	0.899	0.829	0.788	0.779
PBL	0.921	0.911	0.880	0.880	0.870	0.929	0.919	0.888	0.888	0.878
PL	0.951	0.942	0.936	0.921	0.910	0.959	0.950	0.944	0.929	0.918
Time (s)										
CBD [24]	61.402	67.401	78.634	85.458	89.059	55.384	60.796	70.928	77.083	80.331
VRM [35]	62.512	66.859	79.579	87.693	90.170	56.386	60.307	71.780	79.099	81.333
PBL	64.591	69.059	81.287	85.540	91.501	58.261	62.291	73.321	77.157	82.534
PL	65.712	69.108	82.082	85.569	92.369	59.272	62.336	74.038	77.183	83.317

Table 9 Performance measures as average of three image sets for $p > 2$, $\phi = 1$ and $k = 0.5$ with different noise densities

	128 × 128 pixel size					512 × 512 pixel size				
	$\sigma_X = 10$	$\sigma_X = 20$	$\sigma_X = 30$	$\sigma_X = 40$	$\sigma_X = 50$	$\sigma_X = 10$	$\sigma_X = 20$	$\sigma_X = 30$	$\sigma_X = 40$	$\sigma_X = 50$
PSNR										
CBD [24]	27.972	25.295	23.739	22.636	22.352	30.570	27.644	25.943	24.739	24.429
VRM [35]	29.527	28.945	25.896	25.417	23.297	32.270	31.634	28.301	27.778	25.462
PBL	31.771	30.603	29.155	28.408	28.378	34.721	33.445	31.863	31.047	31.014
PL	34.769	34.106	33.331	32.654	32.582	37.999	37.274	36.427	35.688	35.608

Table 9 continued

	128 × 128 pixel size					512 × 512 pixel size				
	$\sigma_X = 10$	$\sigma_X = 20$	$\sigma_X = 30$	$\sigma_X = 40$	$\sigma_X = 50$	$\sigma_X = 10$	$\sigma_X = 20$	$\sigma_X = 30$	$\sigma_X = 40$	$\sigma_X = 50$
MAE										
CBD [24]	4.133	5.322	6.122	7.187	9.416	4.517	5.816	6.691	7.855	10.289
VRM [35]	4.914	5.014	5.929	7.233	8.615	5.369	5.479	6.479	7.905	9.416
PBL	3.012	3.137	4.128	4.914	5.014	3.292	3.428	4.512	5.369	5.480
PL	2.698	2.517	3.132	3.512	4.018	4.321	4.123	4.108	3.838	3.019
SSIM										
CBD [24]	69.559	66.599	63.567	60.670	52.113	76.020	72.786	69.472	66.306	56.954
VRM [35]	71.074	66.780	62.857	58.061	52.997	77.677	72.983	68.696	63.454	57.921
PBL	74.522	70.215	65.612	61.677	58.605	81.445	76.738	71.707	67.406	64.049
PL	77.313	73.884	67.299	64.488	62.371	84.495	80.747	73.550	70.479	68.165
QI										
CBD [24]	0.897	0.866	0.858	0.817	0.778	0.917	0.886	0.878	0.837	0.798
VRM [35]	0.886	0.877	0.807	0.766	0.757	0.906	0.897	0.827	0.786	0.777
PBL	0.907	0.897	0.866	0.866	0.856	0.927	0.917	0.886	0.886	0.876
PL	0.937	0.928	0.922	0.907	0.896	0.957	0.948	0.942	0.927	0.916
Time (s)										
CBD [24]	49.647	54.498	63.580	69.098	72.009	54.259	59.560	69.486	75.516	78.699
VRM [35]	50.544	54.059	64.344	70.905	72.907	55.241	59.081	70.321	77.491	79.680
PBL	52.226	55.838	65.725	69.164	73.984	57.078	61.025	71.831	75.589	80.857
PL	53.132	55.878	66.368	69.188	74.685	58.068	61.068	72.533	75.615	81.623

statistical conditions, is well adapted to characterize images that are effected by Poisson-distributed noise, Gaussian-distributed noise or any other compound distributed noise by varying scale parameter. In the presence of noise, the proposed multi-parameter estimator provides slightly better performance than Bayesian and variational parameter-based estimators. Experimental results on the images show the superiority of proposed denoiser compared to other denoising approaches. This suggests that the proposed method is an accurate model as it is able to restore the contrast, shape, and scale behavior of the of images; this gives the proposed estimator good denoising properties. The experimental results show that the proposed denoiser outperforms the other methods very well especially at low SNRs. The proposed algorithm may be extended to color images and video framework, which may further improve video denoising.

References

1. M. Abramowitz, I.A. Stegun, *Handbook of Mathematical Functions with Formulas Graphs and Mathematical Tables*, 3rd edn. (Dover Publications, New York, 1965)

2. S.K. Bar-Lev, P. Enis, Reproducibility and natural exponential families with power variance functions. Ann. Stat. **14**(4), 1507–1522 (1986)
3. P. Besbeas, I. De Feis, T. Sapatinas, A comparative simulation study of wavelet shrinkage estimators for Poisson counts. Int. Stat. Rev. **72**(2), 209–237 (2004)
4. M.I.H. Bhuiyan, M.O. Ahmad, M.N.S. Swamy, Spatially adaptive thresholding in wavelet domain for despeckling of ultrasound images. IET Image Proc. **3**(3), 147–162 (2009)
5. G.G. Bhutada, R.S. Anand, S.C. Saxena, Image enhancement by wavelet-based thresholding neural network with adaptive learning rate. IET Image Proc. **5**(7), 573–582 (2011)
6. J.M. Borwein, P.B. Borwein, *Pi and the AGM: A Study in Analytic Number Theory and Computational Complexity* (Wiley, New York, 1998)
7. R.P. Brent, *Multiple-Precision Zero-Finding Methods and the Complexity of Elementary Function Evaluation-Analytic Computational Complexity* (Academic Press, New York, 1975), pp. 151–176
8. E. Chouzenoux, A. Jezierska, J.-C. Pesquet, H. Talbot, A convex approach for image restoration with exact Poisson–Gaussian likelihood. SIAM J. Imaging Sci. **8**(4), 2662–2682 (2015)
9. M. Clevenson, J. Zidek, Simultaneous estimation of the means of independent Poisson laws. J. Am. Stat. Assoc. **70**(351), 698–705 (1975)
10. M.P. Eckert, A.P. Bradley, Perceptual quality metrics applied to still image compression. Signal Process. Spec. Issue Image Video Qual. Metr. **70**(3), 177–200 (1998)
11. A.M. Eskicioglu, P.S. Fisher, Image quality measures and their performance. IEEE Trans. Commun. **43**(12), 2959–2965 (1995)
12. S.K.S. Fan, Y. Lin, A fast estimation method for the generalized Gaussian mixture distribution on complex images. Comput. Vis. Image Underst. **113**(7), 839–853 (2009)
13. M.A.T. Figueiredo, J.M. Bioucas-Dias, Restoration of Poissonian images using alternating direction optimization. IEEE Trans. Image Process. **19**(12), 3133–3145 (2010)
14. S. Gai, G. Yang, M. Wan, L. Wang, Hidden Markov tree model of images using quaternion wavelet transform. Comput. Electr. Eng. **40**(3), 819–832 (2014)
15. M. Ghosh, J.T. Hwang, K.W. Tsui, Construction of improved estimators in multiparameter estimation for discrete exponential families. Ann. Stat. **11**(2), 351–367 (1983)
16. B. Girod, *What's Wrong with Mean-Squared Error-Digital Images and Human Vision* (MIT Press, Cambridge, 1993), pp. 207–220
17. K. Hirakawa, P.J. Wolfe, Skellam shrinkage: wavelet-based intensity estimation for inhomogeneous Poisson data. IEEE Trans. Inf. Theory **58**(2), 1080–1093 (2012)
18. Y.M. Huang, M.K. Ng, Y.W. Wen, A new total variation method for multiplicative noise removal. SIAM J. Imaging Sci. **2**(1), 20–40 (2009)
19. H.M. Hudson, A natural identity for exponential families with applications in multiparameter estimation. Ann. Stat. **6**(3), 473–484 (1978)
20. X. Jin, K. Hirakawa, Approximations to camera sensor noise. in *Proceedings SPIE-IS & T , Image Processing: Algorithms and Systems XI*, p. 8655 86550H-1–86550H-7 (2013)
21. J.L. Knight, The joint characteristic function of linear and quadratic forms of non-normal variables. Indian J. Stat. Ser. A **47**(2), 231–238 (1985)
22. E.D. Kolaczyk, R.D. Nowak, Multiscale likelihood analysis and complexity penalized estimation. Ann. Stat. **32**(2), 500–527 (2004)
23. C.E. Lawrence, F.G. Ronald, *Measure Theory and Fine Properties of Functions (Studies in Advanced Mathematics)* (CRC Press, Boca Raton, 1991)
24. T. Le, R. Chartrand, T.J. Asaki, A variational approach to reconstructing images corrupted by Poisson noise. J. Math. Imaging Vis. **27**(3), 257–263 (2007)
25. S. Levine, Y. Chen, J. Stanich, Image restoration via nonstandard diffusion. Department of Mathematics and Computer Science, Duquesne University, Pittsburgh, PA, Technical Report 04-01 (2004)
26. A. Li, D. Chen, K. Lin et al., Nonlocal joint regularizations framework with application to image denoising. Circuits Syst. Signal Process. **35**(8), 2932–2942 (2016)
27. F. Luisier, T. Blu, M. Unser, Image denoising in mixed Poisson–Gaussian noise. IEEE Trans. Image Process. **20**(3), 696–708 (2011)
28. M. Makitalo, A. Foi, Optimal inversion of the generalized Anscombe transformation for Poisson–Gaussian noise. IEEE Trans. Image Process. **22**(1), 91–103 (2013)
29. J.A. Nelder, Y. Lee, Likelihood, quasi-likelihood and pseudolikelihood: some comparisons. J. R. Stat. Soc. Ser. B (Methodol.) **54**(1), 273–284 (1992)
30. J.A. Nelder, D. Pregibon, An extended quasi-likelihood function. Biometrika **74**(2), 221–232 (1987)

31. S. Paul, D.B. Steve, Wavelet denoising of multicomponent images using Gaussian scale mixture models and a noise-free image as priors. IEEE Trans. Image Process. **16**(7), 1865–1872 (2007)
32. M. Protter, I. Yavneh, M. Elad, Closed-form MMSE estimation for signal denoising under sparse representation modelling over a unitary dictionary. IEEE Trans. Signal Process. **58**(7), 3471–3484 (2010)
33. S. Setzer, G. Steidl, T. Teuber, Deblurring Poissonian images by split Bregman techniques. J. Vis. Commun. Image Represent. **21**, 193–199 (2010)
34. S.V. Stehman, R.L. Czaplewski, Introduction to special issue on map accuracy. Environ. Ecol. Stat. **10**(3), 301–308 (2003)
35. G. Steidl, T. Teuber, Removing multiplicative noise by Douglas–Rachford splitting. J. Math. Imaging Vis. **36**(2), 168–184 (2010)
36. G.M. Tallis, R. Light, The use of fractional moments for estimating the parameters of a mixed exponential distribution. Technometrics **10**(1), 161–175 (1968)
37. K.E. Timmermann, R.D. Nowak, Multiscale modeling and estimation of Poisson processes with application to photon-limited imaging. IEEE Trans. Inf. Theory **45**(3), 846–862 (1999)
38. J. Turek, I. Yavneh, M. Protter, M. Elad, On MMSE and MAP denoising under sparse representation modeling over a unitary dictionary. IEEE Trans. Signal Process. **59**(8), 3526–3535 (2011)
39. J.S. Uebersax, A generalized Kappa coefficient. Educ. Psychol. Meas. **42**, 181–183 (1982)
40. A. Veevers, M.C.K. Tweedie, Variance-stabilizing transformation of a Poisson variate by a beta function. J. Roy. Stat. Soc. Ser. C (Appl. Stat.) **20**(3), 304–308 (1971)
41. Z. Wang, A.C. Bovik, A universal image quality index. IEEE Signal Process. Lett. **9**(3), 81–84 (2002)
42. Z. Wang, A.C. Bovik, L. Lu, Why is image quality assessment so difficult. IEEE Int. Conf. Acoust. Speech Signal Proces. Orlando FL. USA **4**, 3313–3316 (2002)
43. T.J. Watson, D.V. Chudnovsky, G.V. Chudnovsky, Approximations and Complex Multiplication According to Ramanujan. IBM T.J, Watson Research Center (1987)
44. R.M. Willett, R.D. Nowak, Multiscale Poisson intensity and density estimation. IEEE Trans. Inf. Theory **53**(9), 3171–3187 (2007)
45. S. Winkler, Perceptual distortion metric for digital color video. Proc. SPIE Hum. Vis. Electron. Imaging IV **3644**, 175–184 (1999)
46. M.V. Wüthrich, Claims reserving using Tweedie's compound Poisson model. ASTIN Bull. **33**(2), 331–346 (2003)
47. H.Y. Yang, X.Y. Wang, T.X. Qua, Image denoising using bilateral filter and Gaussian scale mixtures in shiftable complex directional pyramid domain. Comput. Electr. Eng. **37**(5), 655–667 (2011)
48. S. Yun, H. Woo, A new multiplicative denoising variational model based on mth root transformation. IEEE Trans. Image Process. **21**(5), 2523–2533 (2012)
49. B. Zhang, J.M. Fadili, J.-L. Starck, Wavelets, ridgelets, and curvelets for Poisson noise removal. IEEE Trans. Image Process. **17**(7), 1093–1108 (2008)
50. B. Zhang, J. Fadili, J.-L. Starck, J.-C. Olivo-Marin, Multiscale variance-stabilizing transform for mixed-Poisson–Gaussian processes and its applications in bioimaging. in *IEEE International Conference on Image Processing (ICIP'07)*, vol. 6, p. VI-233–VI-236 (2007)